

Oxygen Disorder Effects in High T_c Superconductors

Y. Bruynseraede, J. Vanacken, B. Wuyts and C. Van Haesendonck

Laboratorium voor Vaste Stof-Fysika en Magnetisme, Katholieke Universiteit Leuven, 3030 Leuven, Belgium

J. -P. Locquet

IBM Research Division, Zürich Research Laboratory, 8803 Rüschlikon, Switzerland

and

I. K. Schuller

Physics Department-B019, University of California-San Diego, La Jolla, California 92093, U.S.A.

Received March 20, 1989; accepted April 11, 1989

Abstract

It is now well established that oxygen plays a crucial role in the structural, magnetic and transport properties of high T_c materials. We present here a brief review of the effect of the oxygen deficiency and vacancy ordering on the superconducting and magnetic properties of various superconductors.

1. Introduction

The physical properties of high T_c oxide compounds are very sensitive to the exact oxygen stoichiometry. Changes in the oxygen content can induce structural transformations, metal-insulator transitions, and variations in the transition temperature below which magnetic ordering and superconductivity are established. For copper oxide-based high T_c superconductors, the oxygen content determines the hole density, the parameter upon which the occurrence of superconductivity seems to depend. The effect of the oxygen content, ordering and kinetics on the physical properties, particularly those related to the superconducting properties of the compound R₂Ba₂Cu₃O_{7-δ} will be discussed in this paper.

Soon after its discovery [1] the YBa₂Cu₃O_{7-δ} (YBCO) structure was studied extensively using X-ray and neutron diffraction [2]. The structural phase transition from an orthorhombic to a tetragonal unit cell was found to be driven by a decreasing oxygen content [3]. Moreover, the oxygen vacancy distribution in the chains and/or planes seemed to be closely related to the appearance of superconductivity [4, 5].

When studying the oxygen kinetics in YBCO, it is important to consider the oxidation reaction as well as the oxygen diffusion process [6, 7]. Using an oxygen evolution technique it is possible to identify desorption kinetics and to calculate the related activation energies [8–11]. On the other hand, oxygen evolution experiments also provide a very sensitive tool to detect impurity phases.

In agreement with the observations by other groups [12–15], we also detected two distinct superconducting phases (90 K and 60 K) when the oxygen content in the YBCO system is reduced. This is probably related to the ordering of the oxygen vacancies in the CuO basal plane [16, 17].

These results may be analyzed in the framework of the valence (or oxidation state) of copper or equivalently the hole density. The formal valence of Cu can be simply modified by

changing the oxygen content: increasing the oxygen content will increase the formal Cu valence and vice versa.

The pairing mechanism in the high T_c superconductivity may be a magnetic mechanism, rather than the conventional electron-phonon interaction in the BCS theory. Evidence for a magnetic pairing mechanism is the switching between antiferromagnetic and superconducting order when the concentration of holes in the conducting CuO₂ planes of the YBCO compound is varied [18]. It has been shown that the increase of the oxygen concentration is closely related to the destruction of the antiferromagnetic order and the appearance of superconductivity [19, 20].

Finally, it is important to develop techniques which can help to characterize the structural properties and chemical composition of thin-film superconductors [21], especially with respect to the overall oxygen stoichiometry, the appearance of oxygen depleted surface layers, and the oxygen ordering. Detailed information about the oxygen stoichiometry in thin films is difficult or impossible to obtain from neutron diffraction, thermogravimetry or chemical methods. We show that Raman scattering is able to determine accurately the oxygen stoichiometry in thin films [22].

2. Structure and oxygen occupancy

The most extensively studied oxide superconductor is the family R₂Ba₂Cu₃O_{7-δ} (R = Y, Nd, Sm, Eu, Gd, D, Ho, Er, Tm, Yb, Lu) because it has a high T_c (> 90 K) and can be made single phase in a reliable and reproducible way.

The structure of the YBCO compound was determined by different groups using X-ray powder, X-ray single crystal and neutron diffraction [2]. The conventional unit cell consists of two dimpled CuO₂ planes separated by an Y layer which contains no oxygen and intercalated with two BaO and one CuO layers (Fig. 1). The CuO layer contains a most striking structural feature: an ordering of the oxygen vacancies giving rise to one-dimensional Cu–O “chains”. The presence of the ordered oxygen vacancies produces a structure with orthorhombic symmetry (*Pmmm*) because of the existence of the Cu–O chains (Cu1–O1 in Fig. 1).

Since a calculation of the formal oxidation state results in an oxygen stoichiometry of 6.5, the presence of more oxygen in the chain sites, produces a total oxygen stoichiometry near

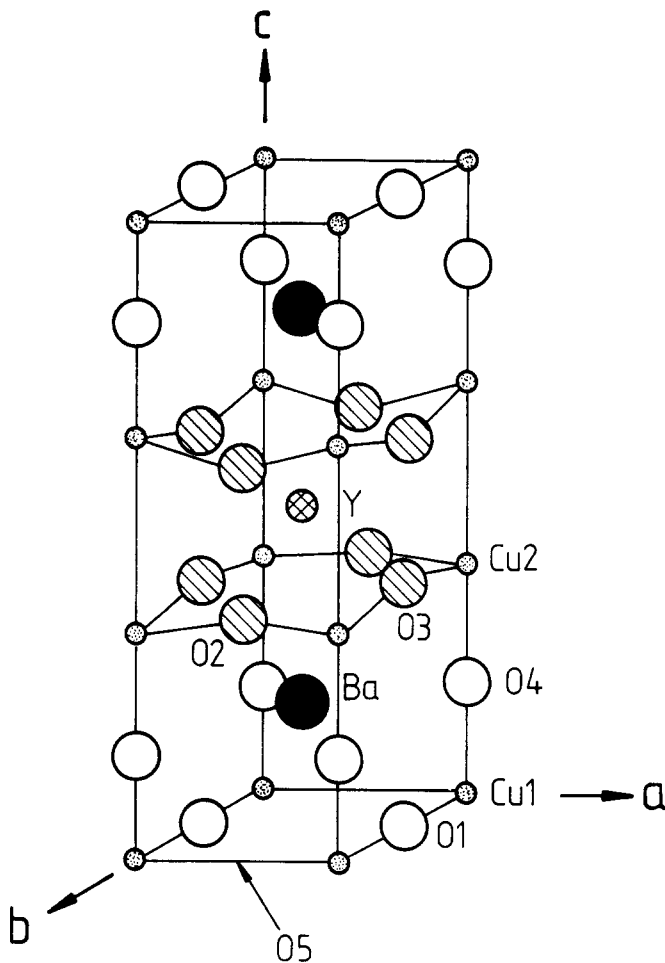


Fig. 1. Orthorhombic structure of the $\text{YBa}_2\text{Cu}_3\text{O}_7$ compound. (From Ref. [3]).

7. This implies that the hole-like carriers are provided by the oxygen in the chains.

Changes in oxygen stoichiometry strongly affect superconductivity in the RBCO system: as oxygen is removed from the chains, some of the remaining oxygen atoms move to sites between the chains, eventually resulting in a transition to a disordered tetragonal structure [3, 4]. T_c drops with decreasing oxygen content and reaches zero near the orthorhombic-to-tetragonal transition which corresponds to a composition near $\text{YBa}_2\text{Cu}_3\text{O}_{6.4}$ [23].

3. Oxygen desorption

3.1 Oxygen mobility

The oxygen bonding in ceramic superconductors can be approached in two different ways. First we can consider the oxidation process in which an oxygen atom is added to the structure or lost from it in thermodynamic equilibrium [6]. This process depends sensitively on the oxygen partial pressure, as experimentally observed by neutron diffraction experiments [15]. Figure 2 shows the dependence of the O1, O5 and O4 site occupancies on oxygen partial pressure for a sample annealed at 490°C . As the oxygen pressure decreases, oxygen is lost from the O1 chain-site, partly filling the O5 site, until the occupancy of both sites equals 0.25. The structure then becomes tetragonal. It is interesting to note that also the occupancy of the O4 site slightly decreases as the oxygen partial pressure is reduced.

The second way of approaching the oxygen mobility is

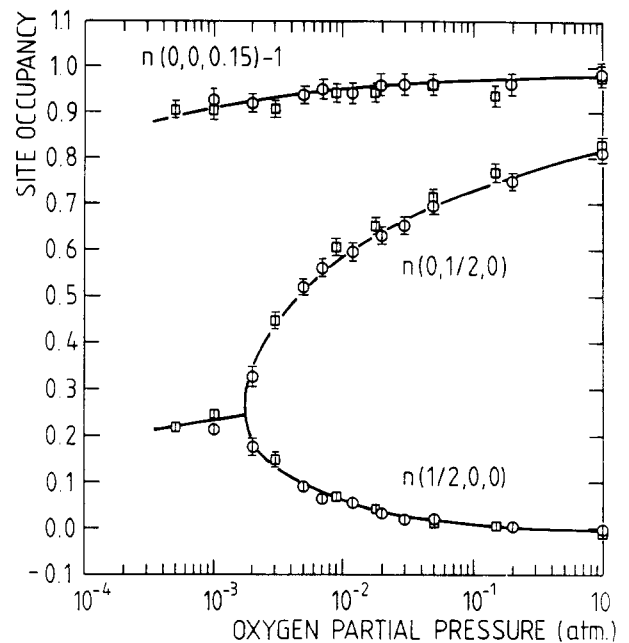


Fig. 2. Occupancy of the O1, O4 and O5 oxygen sites versus oxygen partial pressure for a sample annealed at 490°C . As the oxygen partial pressure decreases, oxygen is lost from the O1 and O4 sites, partly filling the O5 site. (From Ref. [15]).

based on the diffusion process. Since very low heating rates are required to anneal a sample in equilibrium conditions [6], it is often necessary to take into account a diffusion process when studying the effect of temperature on the oxygen content. Classically, thermally activated diffusion can be described using the relation

$$D = D_0[V_{\text{O}}] \exp\left(-\frac{\Delta E}{k_{\text{B}}T}\right) \quad (1)$$

where D_0 is a coefficient including the jump distance and a frequency factor, $[V_{\text{O}}]$ the number of oxygen vacancies and ΔE the energy barrier for a diffusing atoms [24].

Since the diffusion probability is enhanced by oxygen vacancies, we can argue that the O1 oxygen has an important diffusion probability (each O1 has a vacant O5 to jump to). Diffusion of O4 (via O5 positions) is also possible but it will need more energy because its distance to a neighbouring vacancy is larger.

These intuitive arguments are confirmed by the neutron diffraction experiments mentioned above [15], by high temperature Raman measurements [25] and by our own desorption experiments, which are described in detail in the next section.

3.2 Experimental results

The oxygen desorption technique we used for studying the oxygen kinetics in ceramic superconductors [9–11] is in some sense an alternative method for thermogravimetric analysis. In the latter the weight change is recorded during heating, while in our experiments the pressure is measured arising from oxygen desorption from a sample which is mounted in an evacuated closed quartz tube. The mass of our samples was always in the range 10–30 mg and the heating rate $12^\circ\text{C}/\text{min}$. The elevated heating rate implies that the oxygen desorption is dominated by diffusion [Eq. (1)]. In order to rule out spurious effects due to the evolution of impurity gases the evolved gas is analyzed using a mass spectrometer.

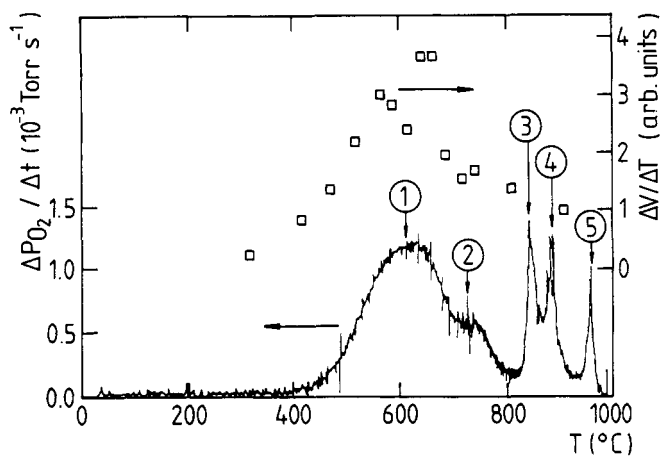


Fig. 3. Evolution curve for an YBCO sample: temperature derivative of the oxygen pressure versus temperature, together with expansion coefficient data from *in situ* neutron diffraction experiments [3]. The different peaks correspond to desorption from several oxygen positions and from impurity phases, as explained in the text.

The data are corrected for measured changes observed in the empty tube due to gas evolution from the walls of the vessel. All those corrections amount to less than 5%. The number of oxygen atoms evolved from the sample can be easily calculated from the measured pressure variation.

Figure 3 shows an evolution curve for a sample with starting stoichiometry near $\text{YBa}_2\text{Cu}_3\text{O}_{6.9}$. The y-axis is directly proportional to the temperature derivative of the number of oxygen atoms evolved from the sample. The open squares in the figure are expansion coefficient data obtained from *in situ* neutron diffraction experiments [3]. The large number of peaks in the evolution curve clearly indicates that several oxygen desorption processes occur at different temperatures. It is possible to assign these processes to different oxygen sites and impurities by using the following arguments.

Comparing ceramics that are known to contain only Cu–O and La–O planes (La_2CuO_4 , $\text{La}_{2-x}\text{Sr}_x\text{CuO}_4$) with samples that contain Cu–O planes and chains, Y or La and Ba–O planes ($\text{YBa}_2\text{Cu}_3\text{O}_{7-\delta}$, $\text{LaBa}_2\text{Cu}_3\text{O}_{7+\delta}$, $\text{Y}_{1-x}\text{Pr}_x\text{Ba}_2\text{Cu}_3\text{O}_{7+\delta}$) and samples with a more complex structure containing Bi–O, Cu–O, Sr–O and Ca planes (Bi–Sr–Ca–Cu–O compounds), we were able to assign the first broad peak in the YBCO spectrum at $\approx 600^\circ\text{C}$ to oxygen evolving from the chains (see Fig. 4) [10]. This identification is confirmed by *in situ* neutron diffraction experiments [3].

We identify the second broad peak at $\approx 720^\circ\text{C}$ (Fig. 3) with oxygen from the O1/O5 site (in the tetragonal phase) together with oxygen from the “bridging” O4 atom. There are several arguments which corroborate this last assumption. First of all, there is the information from neutron diffraction and high temperature Raman measurements from which it is clear that vacancies arise at the O4 site when the oxygen content decreases. Further, following the diffusion arguments given in the previous section, the O4 oxygen has a finite probability to escape by hopping to vacant O1/O5 sites. This process is probably enhanced by the fact that the CuO basal plane becomes positively charged when the oxygen content diminishes and therefore attracts the O4 atoms from the neighbouring BaO planes [17]. Nevertheless, some authors observed only changes in the O1 and O5 content [26].

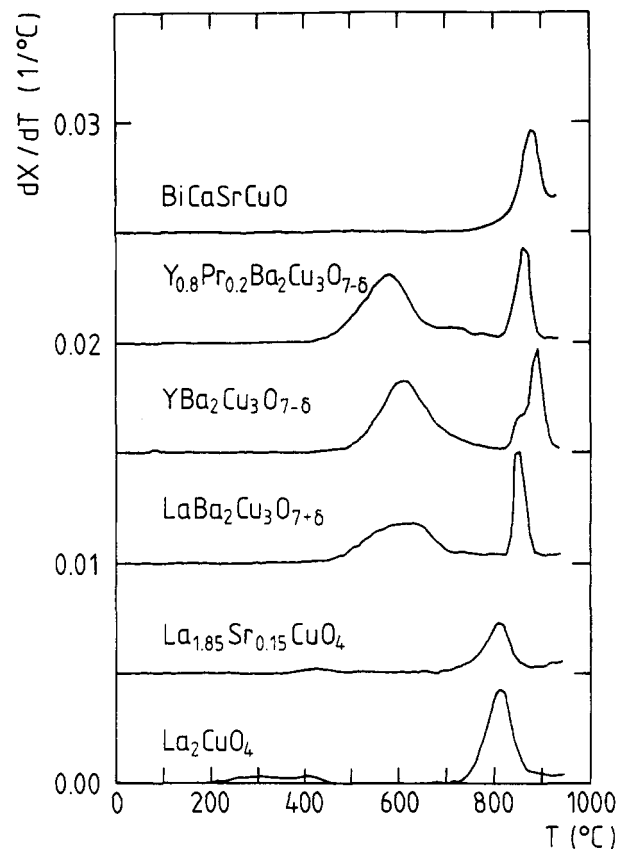


Fig. 4. Comparison of the evolution curves for several ceramics, with or without one dimensional Cu–O sublattices (“chains”).

The high temperature desorption peaks (3, 4 and 5 in Fig. 3) are very sharp and are probably not connected with a diffusion process, but may be due to “sudden” melting processes. By having performed experiments on high-purity samples we can now assign those sharp peaks to a decomposition of impurity phases. This is demonstrated in Fig. 5 where (a) is an evolution curve from an impurity-containing sample and (b) from a very pure sample.

In these experiments the oxygen diffuses via the vacancies until it escapes from the surfaces into the vessel. In this case both the activation energy for diffusion and the activation energy for the escape from the surface (desorption) have to be considered. However as both processes are thermally activated, it is difficult to unambiguously determine, from our limited set of experiments, which process is dominant.

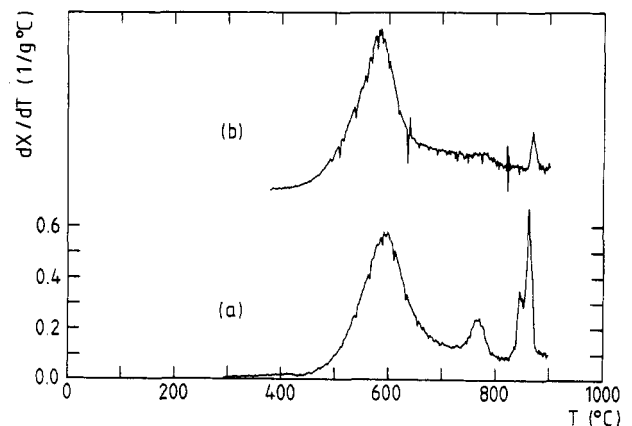


Fig. 5. Comparison of the evolution curves for (a) a sample containing impurities and (b) a very pure YBCO sample.

It is customary to fit first-order desorption experiments from a single site with the relation

$$\frac{dP_{O_2}}{dt} \sim \frac{dN}{dt} \sim (N_0 - N) \exp\left(-\frac{\Delta E'}{k_B T}\right) \quad (2)$$

where P_{O_2} is the oxygen partial pressure, N_0 the initial oxygen content and N the evolved oxygen per unit cell. The energy barrier $\Delta E'$ will be higher than ΔE [eq. (1)] since an escape probability for the internal surface has to be taken into account.

For the low temperature desorption part (first peak at $\approx 600^\circ\text{C}$) we obtain a free energy $\Delta E' \approx 1.2\text{ eV}$. This value is in agreement with work from other groups [27, 28].

4. Oxygen deficiency

4.1 Sample preparation

Numerous groups have reported on the influence of the oxygen content on the superconducting properties of YBCO [29]. At this point it is important to note that different techniques are used to prepare oxygen deficient samples, yielding sometimes different properties. It is obvious that the oxygen vacancy distribution will be less homogeneous in quenched samples than in samples that are carefully (slowly) heated up to a fixed temperature.

We used a 400°C vacuum annealing – starting from high-quality superconducting samples – in order to prepare oxygen deficient samples [11]. This procedure consists of annealing the superconducting, fully oxygenated sample in a vacuum $P \approx 10^{-6}$ Torr at 400°C . The annealing time determines the amount of oxygen losses. By performing a desorption experiment afterwards, it is possible to calculate the oxygen loss relatively to an untreated sample.

4.2 Oxygen vacancy ordering and superconductivity

The oxygen deficient samples have been characterized by X-ray diffraction and their superconducting properties have been studied with a high frequency rf susceptibility method.

A study of the detailed high frequency response is quite revealing, because in this case the signature of two different phases is clearly present. Figure 6 shows a graph of the susceptibility signal for various annealing times at 400°C . The superconductivity is signaled by a sharp peak starting at 92 K, for the samples annealed for less than 1 h. For annealing times between 2 and 6 h the presence of two phases becomes obvious; one around 90 K and another around 60 K. As the annealing time increases, the 60 K signal becomes stronger and the 90 K signal becomes progressively weaker and ultimately disappears. Further annealing gradually destroyed the 60 K phase. The interpretation is straightforward. As the sample is annealed for longer times, the 90 K phase is transformed progressively into the 60 K phase. When the annealing time is further increased, the latter phase is slowly depleted of oxygen and transformed into an insulating phase with vanishing transition temperature.

The evolution of the various phases is therefore consistent with thermodynamic theories which predict a decomposition into two or more distinct oxygen phases [30]. The interesting additional information implied by the present experiments is that there are *two* superconducting phases, with transition temperatures 60 K and 90 K, which give rise to the presence of the plateau in the transition temperature versus oxygen

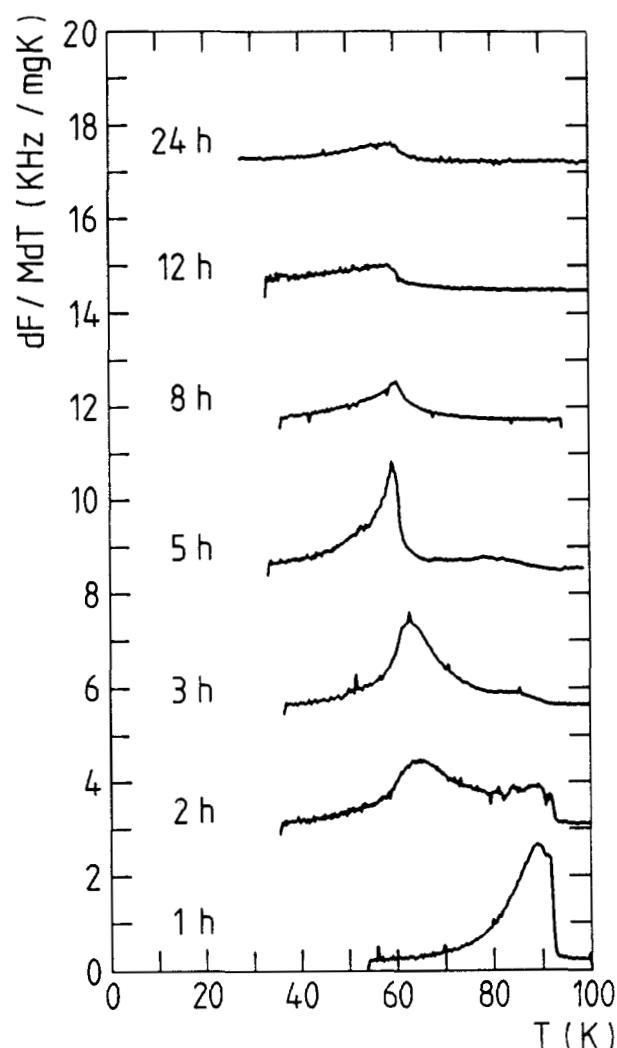


Fig. 6. Susceptibility signal versus temperature for YBCO samples, vacuum-annealed at 400°C for different times. The curves are shifted upwards for clarity.

content graph. Since both phases can coexist it is clear that a resistive measurement of T_c will always be determined by percolating effects. Furthermore the presence of the two phases shows that the picture relating T_c to the hole density is quite too simple.

High resolution electron microscopy can also distinguish between two phases (which might be correlated to the 60 K and 90 K superconducting phases). For complete oxidized samples ($\delta = 0$) the oxygen vacancies are ordered with Cu–O chains parallel to the b-axis. For the ordered $\delta = 0.5$ regions there is a modulation in the a-direction corresponding to the occupancy by oxygen of one out of every two chains [31]. It remains still an open question which superstructure (if needed) determines the 60 K phase.

4.3 Antiferromagnetic ordering

It has been found that magnetic character of the ceramic superconductors is strongly related to the oxygen content [19, 20]. The YBCO system (or in general the RBCO) has been found to become magnetic when superconductivity disappears. In this magnetic regime there are two separate transitions to long range antiferromagnetic order of the Cu spins. The high temperature transition involves the CuO_2 layers and has a Néel temperature $T_{N_1} \sim 500\text{ K}$ at $\delta = 1$ and

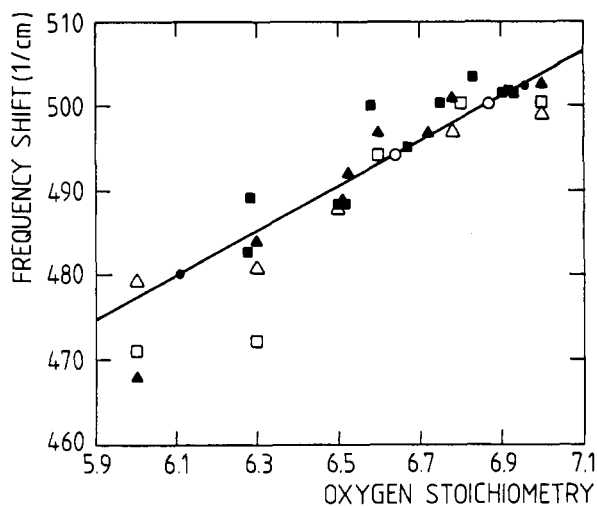


Fig. 7. Dependence of the $\sim 500 \text{ cm}^{-1}$ Raman line on oxygen stoichiometry determined by a number of groups: (■) for Ref. [33], (Δ) from Ref. [34], (\blacktriangle) from Ref. [35], (\blacklozenge) from Ref. [36] and (\square) from Ref. [37]. Two thin-film samples before and after additional annealing are represented by (\circ). The solid line is a least squares fit to all the data.

monotonically decreases to zero for $\delta \sim 0.5$. The low temperature transition involves the ordering of the Cu spins in the "chain" layers and has a Néel temperature T_{N_2} , which is very sensitive to δ and apparently also to other parameters of the sample preparation techniques (e.g. pressure).

These observations of magnetic interactions have stimulated the idea that it might well be a magnetic mechanism which provides the pairing of the charge carriers in these new ceramic superconductors.

5. Thin films

Thin films of the new high T_c copper oxide superconductors have important applications in basic research and technology. A variety of fabrication techniques have been used, particularly electron beam, laser beam and sputter deposition [21].

The correct metal ion stoichiometry in the films can in principle be obtained from a knowledge of the evaporation or sputtering rates. However, the partial oxygen pressure during deposition, rate fluctuations and substrate temperature can seriously affect the final stoichiometry. Determining the absolute oxygen stoichiometry using neutron diffraction data is only possible for large bulk samples [3]. Several techniques such as thermogravimetry [29] and gas evolution [8] can only determine the relative oxygen stoichiometry (by comparison) while X-ray diffraction is not able to determine oxygen. We have shown [22] that room temperature Raman scattering of $\text{YBa}_2\text{Cu}_3\text{O}_{7-\delta}$ thin films provides an excellent speedy and contactless technique for the determination of secondary phases and even the oxygen content of the superconducting phase. It has been reported in the literature [33–37] that the strongest Raman line of YBCO at 500 cm^{-1} arises possibly from vibrations of oxygen located in the O2, O3 or O4 sites. Figure 7 shows the dependence of the $\sim 500 \text{ cm}^{-1}$ line on oxygen stoichiometry determined in bulk samples by a number of groups and in two thin film samples by us [22]. The comparison of data implies that possibly the discrepancies arise mainly from the independent oxygen stoichiometry determination and not from a disagreement on the exact location of the Raman line. The oxygen stoichiometry of the films

extracted from these data ($7 - \delta \simeq 6.64$ and 6.87) is consistent with their measured transition width and temperature. The Raman technique can therefore be used as a relatively simple, quick and non-destructive room temperature test of the quality and uniformity of a superconducting thin film with respect to the oxygen content.

Acknowledgements

We thank M. D. de Leeuw from Philips Research Laboratories in Eindhoven and H. J. Scheel from the Federal Polytechnical School in Lausanne for providing us some very pure YBCO samples. This work is supported by the Belgian I.U.A.P., G.O.A. and the F.K.F.O. Programs and the U.S. National Science Foundation grant number 8803185 (at U.C.S.D.). International travel was provided by a NATO grant. J. V. is a Research Fellow of the Belgian I.W.O.N.L., B. W. is a Research Fellow of the Belgian F.K.F.O., C. V. H. is a Research Associate of the Belgian N.F.W.O.

References

1. Wu, M. K., Ashburn, J. R., Torrey, C. J., Hor, P. H., Meng, R. L., Gao, L., Huang, Z. J., Wang, Y. Q. and Chu, C. W., *Phys. Rev. Lett.* **58**, 908 (1987).
2. For a review of the relevant literature, see Jorgensen, J. D., *Jpn. J. Appl. Phys.* **26**, (supplement 26-3), 2017 (1987).
3. Jorgensen, J. D., *Phys. Rev.* **B36**, 3608 (1987).
4. Schuller, I. K., Hinks, D. G., Beno, M. A., Capone, D. W., Soderholm, L., Locquet, J. -P., Bruynseraede, Y., Serge, C. U. and Zhang, K., *Solid State Commun.* **63**, 395 (1987).
5. Segre, C. U., Dabrowski, B., Hinks, D. G., Zhang, K., Jorgensen, J. D., Beno, M. A. and Schuller, I. K., *Nature* **329**, 227 (1987).
6. Verweij, H., *Ann. Phys. Fr.* **13**, 349 (1988).
7. Bakker, H., Westerveld, J. P. A., Lo Cascio, D. M. R., and Welch, D. O., *Physica C* **157**, 25 (1989).
8. Strauven, H., Locquet, J. -P., Verbeke, O. B. and Bruynseraede, Y., *Solid State Commun.* **65**, 293 (1988).
9. Locquet, J. -P., Strauven, H., Wuyts, B., Verbeke, O. B., Zhang, K., Schuller, I. K., Vanacken, J., Van Haesendonck, C. and Bruynseraede, Y., *Physica C* **153–155**, 833 (1988).
10. Locquet, J. -P., Vanacken, J., Wuyts, B., Bruynseraede, Y., Zhang, K. and Schuller, I. K., *Europhys. Lett.* **7**, 469 (1988).
11. Locquet, J. -P., Vanacken, J., Wuyts, B., Bruynseraede, Y. and Schuller, I. K., To be published.
12. Shi, D., Capone, D. W., Goretta, K. C., Zhang, K. and Goudey, G. T., *Appl. Phys. Lett.* **63**, 5411 (1988).
13. Cava, R. J., Batlogg, B., Chen, C. H., Rietman, E. A., Zahurak, S. M. and Werder, D., *Nature* **329**, 423 (1987).
14. Tranquada, J. M., Cox, D. E., Kunnmann, W., Moudren, H., Shirane, G., Suenaga, M., Zolliker, P., Vaknin, D., Sinha, S. K., Alvarez, M. S., Jacobson, A. J. and Johnston, D. C., *Phys. Rev. Lett.* **60**, 156 (1988).
15. Jorgensen, J. D., Shaked, H., Hinks, D. G., Dabrowski, B., Veal, B. W., Paulikas, A. P., Nowicki, L. J., Crabtree, G. W., Kwok, W. K., Nunez, L. H. and Claus, H., *Physica C* **153–155**, 578 (1988).
16. Zaanen, J., Paxton, A. T., Jopsen, O. and Andersen, O. K., *Phys. Rev. Lett.* **60**, 2685 (1988).
17. Tranquada, J. M., Heald, S. M., Moodenbaugh, A. R. and Xu, Youwen, *Phys. Rev.* **B38**, 8893 (1988).
18. Sinha, S. K., *MRS Bulletin* **XIII** (6), 24 (1988).
19. For a review, see Markert, J. T., Dunlap, B. D. and Maple, M. B., *MRS Bulletin* **XIV** (1), 37 (1989).
20. For a review, see Fisk, Z., Cheong, S. -W. and Johnston, D. C., *MRS Bulletin* **XIV** (1), 33 (1989).
21. For a review, see Laibowitz, R. B., *MRS Bulletin* **XIV** (1), 58 (1989).
22. Yang, K. Y., Homma, H., Lee, R., Bhadra, R., Grimsditch, M., Bader, S. D., Locquet, J. -P., Bruynseraede, Y. and Schuller, I. K., *Appl. Phys. Lett.* **53**, 808 (1988).
23. Cava, R. J., Batlogg, B., Chen, C. H., Rietman, E. A., Zahurak, S. M. and Werder, D., *Phys. Rev.* **B36**, 5719 (1987).
24. Kingery, W. D., Bowen, H. K. and Uhlmann, D. R., *Introduction to Ceramics* 2nd ed., Wiley, New York (1976).

25. McCarty, K. F., Hamilton, J. C., Shelton, R. N. and Ginley, D. S., *Phys. Rev.* **B38**, 2914 (1988).
26. Hewatt, A. W., Capponi, J. J., Chaillout, C., Marezio, M. and Hewatt, E. A., *Solid State Commun.* **64**, 301 (1987).
27. Bakker, H., Welch, D. O. and Lazareth, O. W., Jr., *Solid State Commun.* **64**, 237 (1987).
28. Yeh, N.-C., tu, K. N., Park, S. I. and Tsuei, C. C., *Phys. Rev.* **B38**, 7087 (1988).
29. For a review, see Tarascon, J. M. and Bagley, B. G., *MRS Bulletin XIV* (1), 53 (1989).
30. Khactaturyan, A. G. and Morris, J. W., Jr., *Phys. Rev. Lett.* **59**, 2776 (1987).
31. Alario-Franco, M. and Chaillout, C., *Physica* **C153-155**, 956 (1988).
32. Tarascon, J. M., McKinnon, W. R., Greene, L. H., Hull, G. W. and Vogel, E. M., *Phys. Rev.* **B36**, 226 (1987).
33. Bhadra, R., Brun, T. O., Beno, M. A., Dabrowski, B., Hinks, D. G., Liu, J. Z., Jorgensen, J. D., Nowicki, L. J., Paulikas, A. P., Schuller, I. K., Segre, C. U., Soderholm, L., Veal, B., Wang, H. H., Williams, J. M., Zhang, K. and Grimsditch, M., *Phys. Rev.* **B37**, 5142 (1988).
34. Thomsen, C., Liu, R., Bauer, M., Wittlin, A., Genzel, L., Cardona, M., Schönherr, E., Bauhofer, W. and König, W., *Solid State Commun.* **65**, 55 (1988).
35. Kourouklis, G. A., Jayaraman, A., Batlogg, B., Cava, R. J., Stavola, M., Krol, D. M., Rietman, E. A. and Schneemeyer, L. F., *Phys. Rev.* **B36**, 8320 (1987).
36. Dai, Y., Swinnea, J. S., Steinfink, H., Goodenough, J. B. and Champion, A., *J. Am. Chem. Soc.* **109**, 5291 (1987).
37. Kirillov, D., Collman, J. P., McDevitt, J. T., Yee, G. T., Holcomb, M. J. and Bozovic, I., *Phys. Rev.* **B37**, 3660 (1988).